



Intermolecular Complexes and Molecular Conformations Directed by Hydrogen Bonds: Matrix Isolation and Ab Initio Studies

Jyoti Saini^{1,2*†}, Pankaj Dubey^{1,3†}, Kanupriya Verma^{1,4†}, Ginny Karir^{1,5†}
and K. S. Viswanathan^{1,6*†} 

Abstract | Studies on hydrogen bonding interaction in various systems, involving phenylacetylene (PhAc), propargyl alcohol (PA), borazine (BNH), propargyl amine (PAm) were performed using matrix isolation infrared spectroscopy and supported by ab initio computations. Weak intermolecular interactions of the above mentioned precursors with water, methanol, ether, acetylene and benzene were studied. These systems manifested O–H... π and n - σ^* interactions, such as C–H...O, N–H...O, O–H...O and O–H...N. In several cases the complexes were multiply tethered involving two or more of the above mentioned contacts. Many of the weak complexes exhibited a number of isomers, and the relative importance of the multiple non-covalent contacts resulted in a competition between the various isomers for the global minimum. It was found that subtle changes in the structures of the precursors tilted the balance towards one isomer or the other. Our studies also threw up a systematic method of building possible structures for complex systems starting from the known structures of related simple systems. We also studied the homodimers of PA and BNH. The BNH dimer was particularly interesting as one of its isomers was characterized by a bis-dihydrogen bond. We also studied the influence of hydrogen bonding interactions in determining the conformational landscape and preference in amino acids. Here again we were able to draw some generalizations regarding the conformational stability of amino acids. The combination of matrix isolation and ab initio computation is a powerful tool for studies on weak intermolecular interactions and conformations.

Keywords: Matrix isolation, Ab initio, Phenylacetylene, Propargyl alcohol, Borazine, Amino acids, Hydrogen bonding, Conformations

1 Introduction

Intermolecular interactions play a key role in deciding the structure and chemical reactivity of materials and their properties. While the strong interactions, such as covalent and ionic bonding, determine the structure of individual molecules, the intermolecular interactions, usually non-covalent in nature, influence supramolecular architectures. Plenty of examples

abound in chemistry, biology, atmospheric chemistry, etc., where the non-covalent interactions assert their importance. Cliched examples are the structure of water, proteins, DNA, graphite, which owe their edifice to these interactions. The study of non-covalent interactions has, therefore, attracted a great deal of interest for almost a century.

All authors contributed equally to the work.

¹ Department of Chemical Sciences, Indian Institute of Science Education and Research, Mohali, Punjab 140306, India.

² Present Address: Sardar Vallabhbhai National Institute of Technology, Surat, Gujarat 395007, India.

³ Present Address: Indian Institute of Technology Gandhinagar, Palaj, Gujarat 382355, India.

⁴ Present Address: Department of Industrial and Physical Pharmacy, Purdue University, West Lafayette, USA.

⁵ Present Address: Department of Inorganic Chemistry, Indian Institute of Science, Bengaluru 50012, India.

⁶ Present Address: Indian Institute of Science Education and Research, Mohali 140306, India.

*jyotisaini@iisermohali.ac.in vish@iisermohali.ac.in kvish53@gmail.com

The non-covalent interactions come in a variety of hues: hydrogen bonding, carbon bonding, halogen bonding, dihydrogen bonding, pnictogen bonding, to name a few.^{1–4} These interactions are characterized by energies that range from about 1 to a few tens of kcal/mol, which is many-folds smaller than the strong covalent or ionic interactions. In spite of their lower stability, these non-covalent interactions are still extremely important because of their cooperativity; i.e., many of the weak interactions work together and hence their energy budget is significant. For example in water (ice), each water molecule is bound to four other molecules, and each water molecule in this conglomeration interacts with other water molecules, thus extending the structure. It is this network of interaction acting in tandem that causes water to have a high boiling point, heat of vaporization and specific heat. This phenomenon of cooperativity has also been popularly referred to as the “Gulliver effect”.

Theoretical models to understand these interactions date back to the beginning of the last century. Of the various non-covalent interactions, hydrogen bonding interaction was the first to be seriously addressed. The first description of weak interactions came probably from Latimer and Rodebush.⁵ Around that time, Huggins⁶ had also alluded to the presence of these weak interactions in his dissertation and referred to them as “hydrogen bridges”. Latimer and Rodebush had presented a picture of a hydrogen atom held between two “oxygen octets”, a picture that is retained even today, when describing these bonds. The term “hydrogen bond” was coined later by Linus Pauling while describing the nature of the bond in $[\text{H}-\text{F}-\text{H}]^-$.⁷ In his book on “The nature of the chemical bond”,⁸ Pauling promoted the concept of relative electronegativities being an important factor in the description of hydrogen bonding. More general definitions were presented later by Pimentel and McClellan⁹ in 1960 and by Steiner in 2002.¹⁰ However, many examples of hydrogen bonding interactions emerged which did not precisely fit into the models described earlier. This warranted a redefinition of the hydrogen bond, which was presented by the IUPAC task force in 2011.¹¹ In recent times, the importance of other non-covalent interactions has also been recognized.

These non-covalent interactions pose a challenge in experimental studies because of their small stabilization energies and also the fact that they work cooperatively. Several experimental

methods have been devised to study these interactions, such as calorimetric studies, X-ray crystallography, spectroscopic studies in condensed media and in cold isolated molecule conditions. In addition, interest has also been generated in studying the dynamics of hydrogen bond formation and dissociation, since these are important aspects in the behavior of many chemical and biological systems. These dynamics are ultrafast processes and ultrafast spectroscopy has, therefore, become the technique of choice for such studies.

These weak interactions not only direct supramolecular architecture but quite often also determine conformational preferences. Factors that direct conformational stabilities are stereoelectronic effects (such as anomeric effects) and steric effects. However, very often, intramolecular non-covalent interactions play a crucial role in stabilizing certain conformations. The role of these weak interactions in the conformational landscapes of amino acids and other biological systems is both interesting and important and hence has been an area of intense interest.

In this article, we will describe the studies on hydrogen bonding interactions using cold molecule techniques. There are two different experimental methods that are adopted in studies using cold molecule spectroscopy. One is the supersonic beam method, where cold molecules are prepared by expanding a gaseous sample from a high pressure region (typically a few atmospheres) to a low pressure region (typically 10^{-7} mbar). Translationally cold molecules are initially prepared in the expansion; other degrees of freedom such as rotations and vibrations then equilibrate with this translationally cold bath and drop their respective temperatures during the expansion. The rates of rotational cooling being significantly higher than vibrational cooling, the resultant ensemble is defined by different characteristic temperatures; $T_{\text{trans}} < T_{\text{rot}} < T_{\text{vib}}$. Typically, these temperatures range from a few K to a few tens of K.¹² At these low temperatures, complexes with weak intermolecular interactions can survive and can be experimentally probed. Furthermore, in the expanded beam, the number density being small, collisions are infrequent which allows weak complexes to survive. A variety of techniques such as FT-microwave, FT-infrared and laser-based methods have been used to study these weak complexes.

Alternatively, cold molecules can also be prepared by a brute force method by cooling a cold finger using a cold cycle He-compressor cooled cryostat onto which the molecules of interest can be deposited to prepare cold molecules. Usually,

the molecules of interest are deposited in an excess of inert gas to achieve molecular isolation—a technique referred to as matrix isolation. The inert gas being in excess, the molecule under study is trapped isolated resulting in a cold, isolated molecule condition.

While both matrix isolation and molecular beam methods probe cold, isolated molecules, the two methods enjoy different characteristics that actually complement each other. Examples of such complementarity will be presented in this article.

This article will basically review the work done in our group on weak intermolecular interactions using the technique of matrix isolation infrared spectroscopy and will draw comparisons with other related works, wherever possible. Important lessons learnt in the process will be discussed during the course of this presentation.

2 Experimental Method

Matrix isolation experiments were performed at a cold finger temperature of ~ 12 K. The cryogenic temperature was attained using closed cycle He-compressor cooled cryostat, CH-202W/HC-4E1 (Sumitomo Heavy Industries Ltd.). N_2 and Ar (Grade-I, Sigma Gases and Services 99.999% pure) were used as matrix gases. A KBr window was mounted on the cryotip on which the matrix was deposited. The cryosystem was housed in a vacuum chamber, where the pressure was typically 10^{-6} mbar, the low pressures being obtained by a diffusion pump (Edwards Diffstack MK2) backed by a rotary pump.

All the samples that were used in our studies on non-covalent interactions were of purities 99% or better and were used without any further purification. However, before use, all the samples were subjected to several freeze–pump–thaw cycles. Vapors of the samples under study were mixed with a large excess of the inert matrix gas, to obtain a typical sample to matrix gas ratio of 1:1000. When interactions between two different molecules were studied, say A and B, the ratios of A:B:Matrix gas were typically 1:1:1000. In addition, concentration dependence studies were also necessarily performed, with the concentrations of each species, A and B, being varied independently, to attain sample to matrix ratios for each species of 1:1000 to 5:1000. Concentration variations are a necessary aspect of the experiments to ascertain the stoichiometry of the weak complexes that are prepared. The concentration of the species, A and/or B in the gas mixture is controlled by maintaining the temperature of the

liquid samples, A and B, at an appropriate temperature so that the vapor pressure of the sample above the liquid would yield the expected sample to matrix ratios. The prepared gas mixture is then expanded through an effusive nozzle into the vacuum system and allowed to deposit on the cryotip, at a typical flow rate of ~ 3 mmol/h. A typical deposition lasts for about an hour. After deposition, a spectrum of the deposited species is recorded using a Bruker Tensor 27 FTIR spectrometer operated at a resolution of 0.5 cm^{-1} . Typically, 8–16 scans were coadded which results in a spectrum with a good signal to noise ratio. After recording a spectrum, the matrix is warmed to a temperature of ~ 25 K for N_2 and ~ 30 K for Ar. The cryotip is held at this elevated temperature for about an hour and then cooled back to the original temperature of ~ 12 K; a process referred to as annealing. A spectrum of the matrix thus annealed is again recorded. The process of annealing is done to encourage diffusion of the trapped species so that a small fraction of the co-deposited species, A and B, can have chance encounters to form a complex. The formation of the complex is identified by the observation of new product features on annealing when compared with the spectra recorded before annealing. Of course, in an annealing process, not only heterodimers, A \cdots B, but also homodimers, A_2 and B_2 can be produced. However, through cleverly designed concentration dependence experiments, the features can be unambiguously assigned to the respective species.

A few experiments were also performed, where the effusive nozzle was replaced by a supersonic nozzle. In the experiments, the stagnation pressure of the gas mixture containing, the samples, A and/or B and the matrix gas in the ratios of say, 1:1:1000, was maintained at ~ 1 atm. Expansion under these conditions produced a supersonic beam which was then deposited on the KBr cryotip. These experiments were different from the experiments performed using an effusive nozzle, because with the effusive nozzle, the complexes were prepared on annealing, while in the supersonic beam experiments, the complexes were prepared in the expansion process, which were then trapped on the cryotip. A combination of such experimental techniques often proved useful in assigning the features of the complexes. This combination of deposition techniques is particularly useful in the study of conformations, the most striking example being our earlier study on trimethyl phosphate.^{13,14}

It is probably important at this point to compare the results that one obtains with molecular

beams with that obtained using the matrix isolation technique. In the beam, the complexes are prepared in cold isolated molecule environments. During the preparation of the complex, orientation of the approaching species is not under control which can give rise to several isomers of the complex. However, the complex once formed usually interconverts to the lowest energy form, the global minimum, which is what is generally observed in these experiments. In the matrix, the complexes are formed by the chance encounter of the participating species and over which one has no control. The various isomers formed in this case, are, however, encapsulated in the matrix cage and due to the operation of the matrix cage it is possible to obtain the different isomers of the complex, since isomer interconversion is precluded due to the operation of the cage effect. The cage effect, therefore, makes it possible to observe local minima, (together with the global minimum structure), which is a highlight of the matrix isolation technique. The combination of the molecular beam and matrix isolation spectroscopy is a very powerful tool in the study of weak complexes, as will become apparent from the discussions presented in this article.

3 Computations

The experimental data obtained using the techniques described above will be almost worthless without support of electronic structure calculations to aid in the assignment of the spectral features. Hence, we used the Gaussian suite of programmes¹⁵ to perform ab initio computations to first arrive at the structures and energies of the precursors and the various isomers of the intermolecular complexes. From the energies of the individual precursors and the complexes, the interaction energies of the complexes were arrived at by subtracting the sum of the energies of the monomeric precursors from the energy of the complex. These computations were usually performed using MP2 and M06-2X methods together with double zeta aug-cc-pVDZ basis sets. When computing the interaction energies, corrections for zero-point energies and basis set superposition errors (BSSE) were also applied using the counterpoise method of Boys and Bernardi.¹⁶ All calculations using the M06-2X method were performed using opt=tight and int=ultrafine options. Single point energy calculations were also calculated at the CCSD(T)/aug-cc-pVDZ level using the geometries obtained at the MP2/aug-cc-pVDZ level. Interaction energies at the complete basis set (CBS) limit were

also calculated using the two-point extrapolation method of Helgaker et al.¹⁷

Vibrational frequency calculations were performed on the precursors and all the isomers of the complexes. The harmonic vibrational frequency calculations were used to ensure that the structure of the complexes obtained did indeed correspond to minima on the potential energy surface, by ensuring that all vibrational frequencies had real eigenvalues. The computed frequency values were also used to assign the observed features in the matrix isolation experiments. All the computed values were scaled appropriately to facilitate the assignment process, using the method of mode-by-mode scaling. Details as to how the scaling factors were computed are discussed in detail in many of our earlier publications.^{18–21} The computed wavenumbers together with the intensities of the various vibrational modes were used to simulate a vibrational spectrum using the SYNSPEC program,²² assuming a Lorentzian line profile with a full-width-half-maximum (FWHM) of 1.0 cm^{-1} .

Atoms-in-molecules (AIM) theory of Bader was implemented through AIM2000 (Version 1.0), on the optimized geometries of the various complexes to obtain the electron densities $\rho(\mathbf{r}_c)$ and the Laplacian $\nabla^2 \rho(\mathbf{r}_c)$ (defined as the sum of the Hessian eigenvalues, $\lambda_1, \lambda_2, \lambda_3$) at the bond critical points corresponding to the non-covalent interaction.^{23, 24} Natural bond orbital (NBO) studies were also performed on the complexes to understand the role of the various electron delocalization interactions.²⁵ Localized molecular orbital energy decomposition analysis (LMO-EDA) using GAMESS was also done to understand the nature of the interactions in each of the complexes.²⁶

4 Discussion

We will discuss a number of hydrogen-bonded systems that can manifest both an $n-\sigma^*$ and H- π contacts and the competition that ensues between them. The systems that will be discussed include non-covalently bonded complexes of phenylacetylene (PhAc), propargyl alcohol (PA), propargyl amine (PAm) and borazine (BNH), studied using matrix isolation infrared spectroscopy.

4.1 Acetylenic Systems: Phenylacetylene, Propargyl Alcohol and Propargyl Amine systems

The first system that we will consider is the phenylacetylene–water system (PhAc–H₂O).¹⁸ This system presents three isomeric structures for the

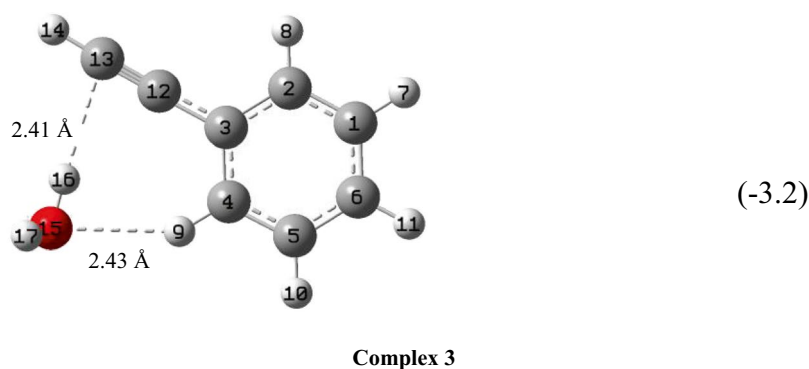
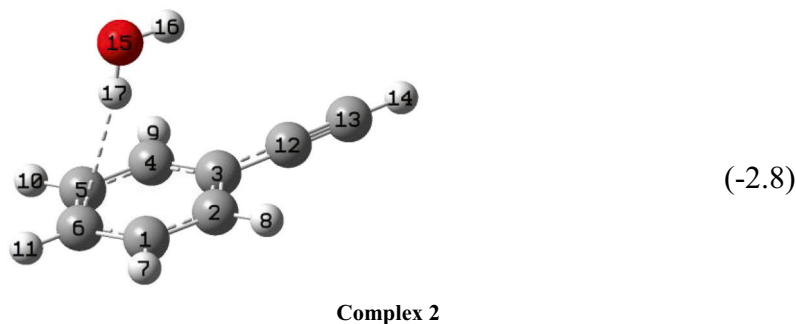
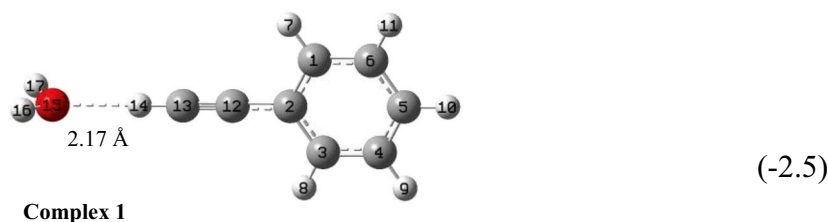


Figure 1: Optimized structures of 1:1 PhAc–H₂O complexes at MP2/aug-cc-pVDZ level. BSSE corrected interaction energy of each complex, in kcal/mol, computed at the same level is given alongside, in parenthesis. (Reproduced from Ref. ¹⁹ with permission).

hydrogen-bonded systems, as shown in Fig. 1. One of these structures has an $n-\sigma^*$ contact, where the acetylenic hydrogen interacts with the lone pair on oxygen of H₂O (Complex 1), i.e., a $\equiv\text{C}-\text{H}\cdots\text{O}$ interaction. The two other structures involve H– π contacts: one where the O–H of water interacts with the phenyl π cloud (complex 2) and another where the O–H of water interacts with the acetylenic π cloud (complex 3). As can be seen from Fig. 1, complex 3 represents the global minimum, while structures 2 and 1 are local minima given in order of decreasing stability. The PhAc–H₂O system was also studied in molecular beams by Arunan et al.²⁷ and Patwari et al.²⁸ who observed the global minimum structure

(Complex 3). The structure corresponding to the $n-\sigma^*$ contact, a local minimum, was not observed in these experiments. In the matrix isolation experiments, a technique known for its ability to trap local minima,²⁹ complex 1 was unambiguously observed. This structure is identified through the large red shift, of $\sim 60\text{ cm}^{-1}$, in the $\equiv\text{C}-\text{H}$ stretch of PhAc in the complex, as shown in Fig. 2.¹⁸ The matrix isolation experiments could not observe the spectral features of the global minimum as the features due to $\equiv\text{C}-\text{H}$ stretch in the complex (as well those of complex 2) had very small computed red shifts, of 2 to 4 cm^{-1} , and were likely overlapped with the feature of the $\equiv\text{C}-\text{H}$ stretch of uncomplexed PhAc.

However, it must be emphasized that the beam studies together with the matrix isolation experiments allows one to probe the potential energy surface of the weak complexes more extensively.

It may be argued that the structure corresponding to the global minimum computed above corresponds to the structure in vacuum and hence may be relevant only to gas phase experiments. In the matrix, interaction with the inert gas may likely cause a change in the energy ordering of the complexes due to the general solvent effect and hence the structure observed in our matrix experiments may in fact correspond to the global minimum in the matrix. To address this point, we performed calculations of the energy of the various PhAc–H₂O complexes by including the solvent effect using the Onsager Self Consistent Reaction Field (SCRf) continuum model. However, introducing the solvent effect preserved the energy ordering of the complexes observed in vacuum.^{18,32}

It would be relevant to note at this point that earlier work indicated the $n\text{-}\sigma^*$ complex to be the global minimum in the C₂H₂–H₂O system;^{30,31} a result that is different from that observed in the PhAc–H₂O system. The difference in behavior in the two complexes can be attributed to the presence of a possible secondary interaction in the PhAc–H₂O complex, between the phenyl hydrogen placed ortho to the acetylenic group in PhAc and the oxygen atom of H₂O, i.e., a C–H...O interaction, as shown in Fig. 1. Such an influential secondary interaction is not possible in the C₂H₂–H₂O complex which consequently results in the $n\text{-}\sigma^*$ complex to be the global minimum. These studies, therefore, highlight the importance of the multiple interactions, where possible, in determining the energy ordering of isomers of the weak complexes.

To confirm if the role of secondary C–H...O interaction is universal, we computationally studied the weak complexes of a few substituted acetylenes with water, which are shown in Fig. 3.³² The systems studied were: propyne–H₂O, but-1-yne–H₂O and but-1-en-3-yne–H₂O, which were compared with C₂H₂–H₂O, PhAc–H₂O and C₆H₆–H₂O. It can be seen that in all the systems, where a secondary C–H...O interaction was possible, the O–H... π interaction was the global minimum, thereby confirming the importance of secondary interactions in the architecture of these weak complexes. That secondary C–H...O interaction present in these complexes was confirmed by an AIM analysis, which indicated the presence of the appropriate bond critical points. The lack of such a secondary interaction in C₂H₂–H₂O

system tilts the balance in favour of the $n\text{-}\sigma^*$ interaction.

Another system that resembles the PhAc–H₂O system is the propargyl alcohol (PA)–H₂O system, and it would be appropriate to discuss this system at this point. The PA–H₂O system, where the PA is restricted to be in the gauche conformation, manifests five isomeric complexes, as shown in Fig. 4.²⁰ There are two nearly degenerate isomeric structures (complexes 1 and 1*) which correspond to the global minima. These isomers have an O–H...O contact with the O–H of PA being the proton donor and the oxygen atom of H₂O serving as the proton acceptor, while the O–H of water makes a π contact with PA. As in the PhAc–H₂O system, PA–H₂O complex also has a local minimum with a $\equiv\text{C}\text{-H}\cdots\text{O}$ contact (Complex 3). The structures 1 and 1* are reminiscent of the global minimum of PhAc–H₂O complex, excepting that the weak C–H...O secondary interaction in PhAc–H₂O is replaced by a much stronger O–H...O contact in PA–H₂O; to an extent the O–H...O contact now serves as the primary interaction. Consequently, the energy difference in the BSSE corrected interaction energies, computed at the MP2/aug-cc-pVDZ level, between the O–H... π and $\equiv\text{C}\text{-H}\cdots\text{O}$ structures in PA–H₂O system ($\Delta = \sim 3.5$ kcal/mol) is significantly larger than in the PhAc–H₂O system ($\Delta = \sim 0.7$ kJ/mol), so much so that the local minimum $\equiv\text{C}\text{-H}\cdots\text{O}$ structure is not even observed in our experiment. Only the features of the near-degenerate global minima structures were observed in our experiments (Fig. 5), the product features being marked with an asterisk.

In structures where multiple contacts are possible, we found that the system adopts a structure, where the distances and angles involved in each of the intermolecular interactions in the multiply tethered complex, are not held at the typical values for such contacts, when they occur alone. The hydrogen bond distance and angles in the complex are compromised somewhat but in such a manner that together they provide the strongest stabilization for the complex. This aspect, referred to as antagonism, has been discussed in detail in our work on PA–H₂O complex.²⁰ A similar phenomenon was also observed in the PA–Methanol complexes.³³ Hydrogen-bonded complexes with multiple interactions were also observed in the PA dimer system.^{34,35}

Studies on the PhAc–C₂H₂ system yielded four minima on the potential surface which are shown in Fig. 6.¹⁹ As is evident from the figure, three of these minima show $\equiv\text{C}\text{-H}\cdots\pi$ contacts, while one structure manifests a $\pi\cdots\pi$ interaction.

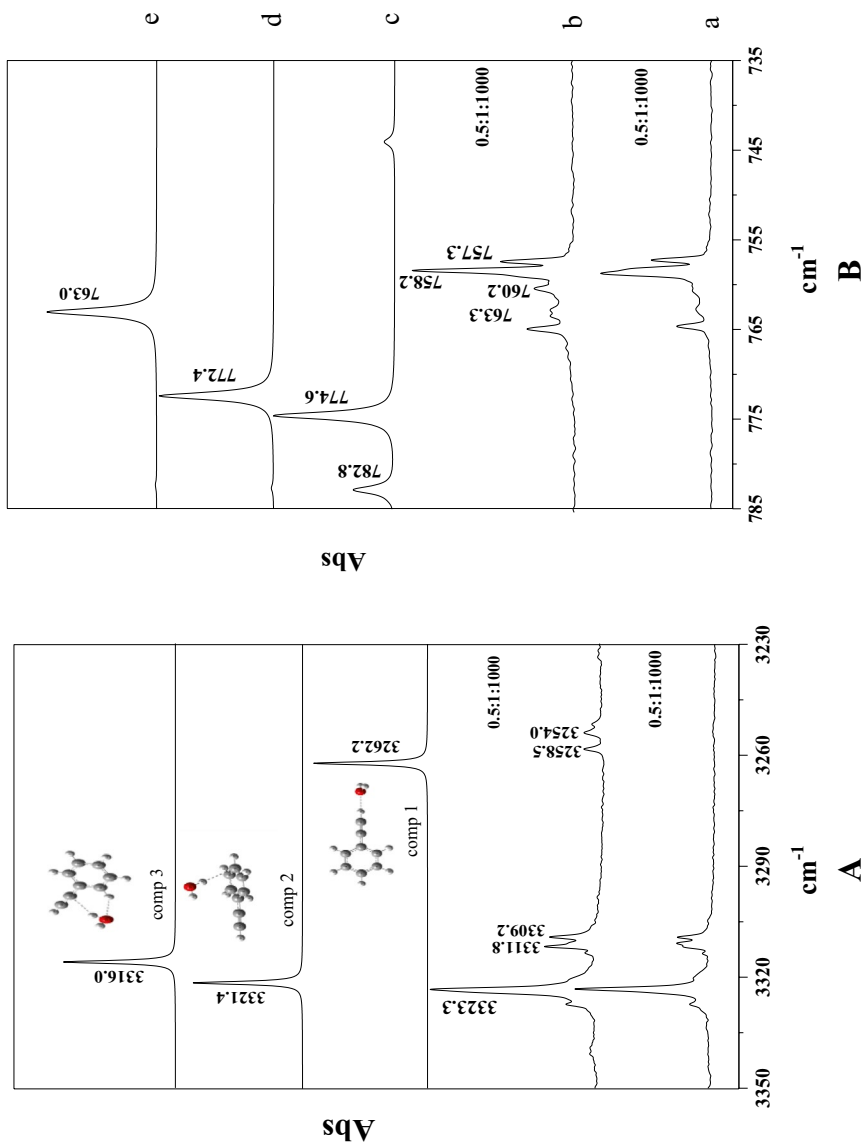


Figure 2: Experimental and computed IR spectra of PhAc–H₂O over the spectral regions **(A)** 3350–3230 cm^{-1} (\equiv C–H stretch of PhAc) and **(B)** 785–735 cm^{-1} (phenyl out-of-plane bend of PhAc) (a) experimental spectrum (PhAc:H₂O:N₂:0.5:1:1000 recorded at 12 K; (b) spectrum of (a) annealed at 27 K; (c) Computed spectrum of Complex 1; (d) computed spectrum of Complex 2; (e) computed spectrum of Complex 3. (Reproduced from Ref. ¹⁴ with permission).

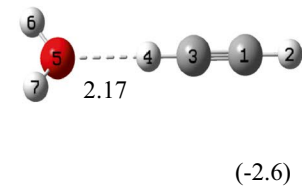
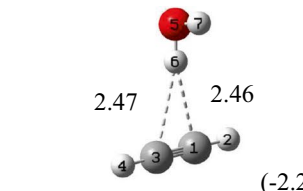
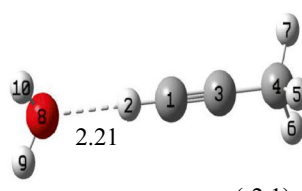
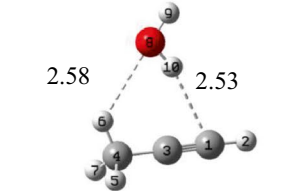
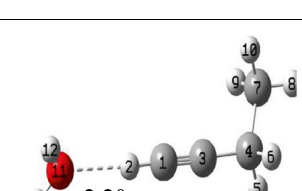
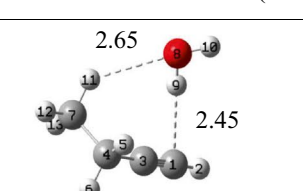
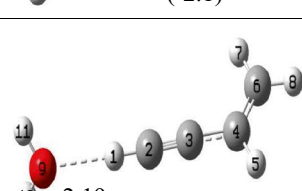
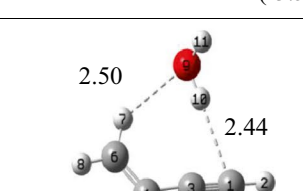
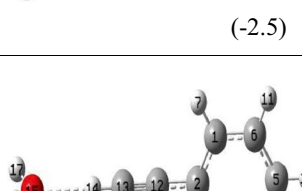
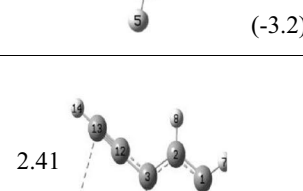
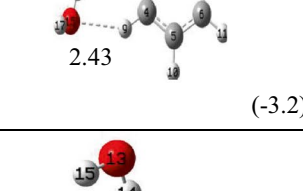
System	$n \cdots \sigma^*$	$H \cdots \pi$
Acetylene-H ₂ O	 2.17 (-2.6)	 2.47 2.46 (-2.2)
Propyne-H ₂ O	 2.21 (-2.1)	 2.58 2.53 (-3.3)
But-1-yne-H ₂ O	 2.20 (-2.1)	 2.65 2.45 (-3.5)
But-1-en-3-yne-H ₂ O	 2.19 (-2.5)	 2.50 2.44 (-3.2)
Phenylacetylene-H ₂ O	 2.17 (-2.5)	 2.41 2.43 (-3.2)
Benzene-H ₂ O		 2.50 (-2.9)

Figure 3: Optimized structures of the various water complexes, obtained at MP2/aug-cc-pVDZ level of theory. Hydrogen bond distances are shown in Å. BSSE corrected interaction energies, in kcal/mol, are given in parenthesis.

The energy difference between the various isomers is rather minimal. Experimentally though, we observed only one structure (complex 3), in which C₂H₂ was the proton donor to the

acetylenic π system of PhAc. AIM and NBO analysis indicated that in this structure, there was a weak secondary interaction between C–H of phenyl and the π cloud of C₂H₂, again pointing to the

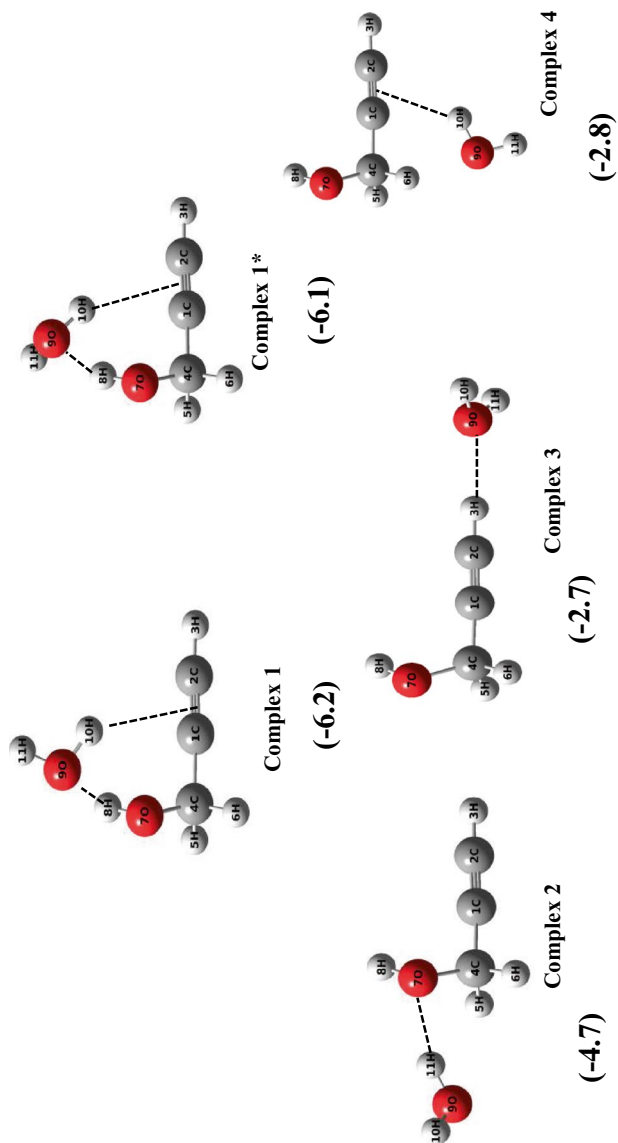


Figure 4: Optimized geometries of the complexes of gauche-PA and H₂O, computed at the MP2/aug-cc-pVDZ level. (Dotted lines do not imply bond paths; these lines are drawn to indicate interactions in the complex). BSSE corrected interaction energies of each complex, in kcal/mol, computed at the MP2/aug-cc-pVDZ level, is given under each structure, in parenthesis. (Reproduced from Ref. 50 with permission).

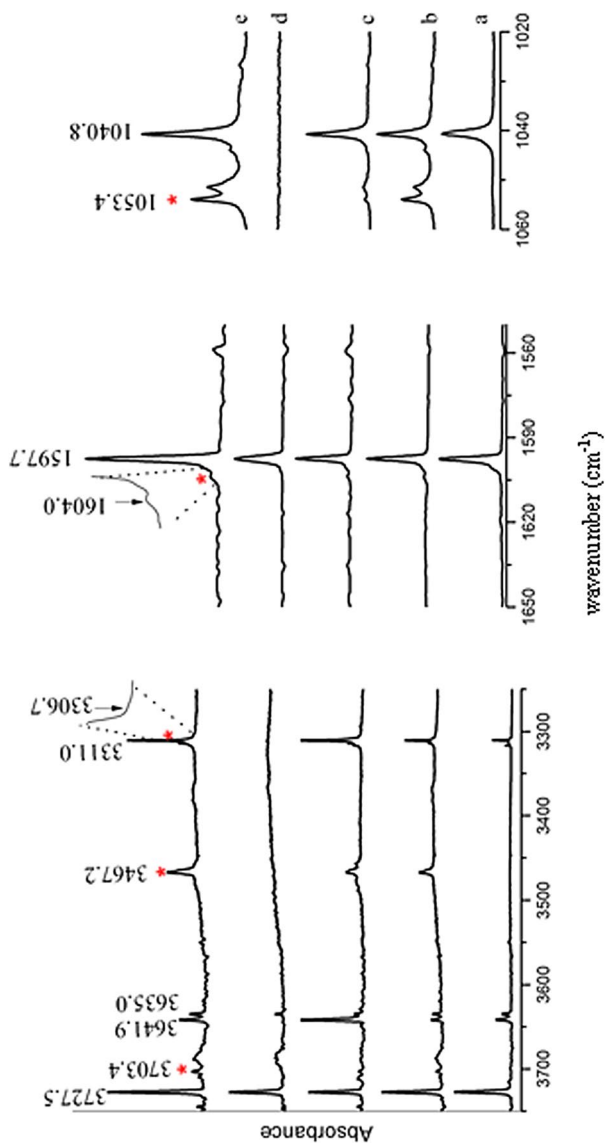


Figure 5: Infrared spectra of PA:H₂O in a N₂ matrix over the regions 3750–3250 cm⁻¹, 1650–1550 cm⁻¹, 1060–1020 cm⁻¹ of a, PA:H₂O:N₂ (0.8:1.0:1000) at 12 K; b, PA:H₂O:N₂ (0.8:1.0:1000) annealed at 30 K; c, PA:H₂O:N₂ (0.8:0.0:1000) annealed at 30 K; d, PA:H₂O:N₂ (0.0:0.5:1000) annealed at 30 K; e, PA:H₂O:N₂ (3.0:0.4:1000) annealed at 30 K Product bands have been marked with an asterisk. (Reproduced from Ref. ⁵⁵ with permission).

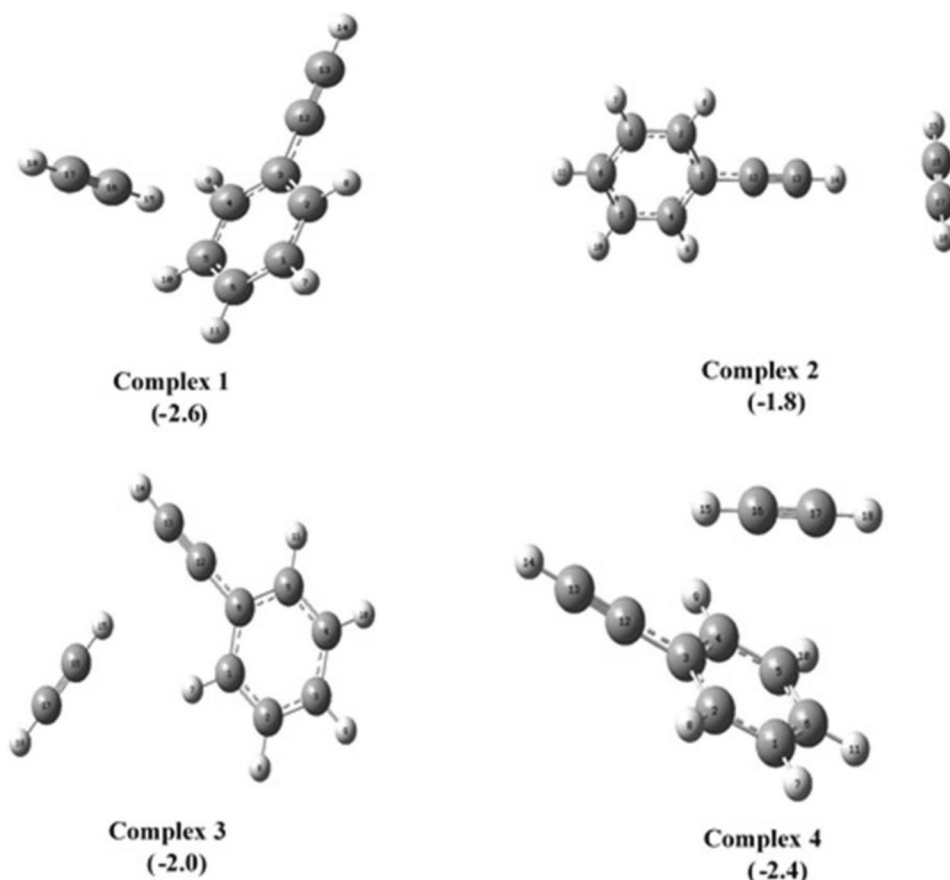


Figure 6: Optimized geometries of PhAc-C₂H₂ complexes. BSSE corrected interaction energies, in kcal/mol, computed at the MP2/aug-cc-pVDZ level is given below each structure, in parenthesis. (Reproduced from Ref. ¹⁰ with permission).

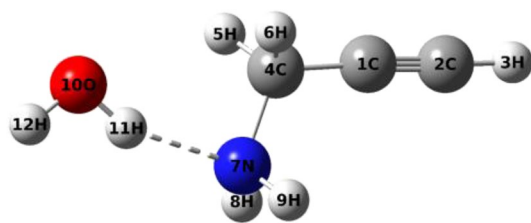


Figure 7: Global minimum structure for the PAm-H₂O complex computed at the MP2/aug-cc-pVDZ level.

role of secondary interactions in determining the stability of weak complexes.

We also studied the 1:1 hydrogen-bonded complexes of propargyl amine (PAm) with H₂O. The global minimum in this system involved an O-H...N interaction, where PAm serves as a proton acceptor and H₂O as the proton donor (Fig. 7).³⁶ This was evident from the observed large red shift of 346.0 cm⁻¹ in the bonded O-H stretch of H₂O subunit from the O-H

antisymmetric stretch in uncomplexed H₂O. Interestingly, this system did not show the global minimum structure shown by PA-H₂O (complex 1 and 1* in Fig. 4), as the N-H group in PAm, unlike the O-H in PA, is a relatively poor proton donor and does not succeed in stabilizing such a structure. The PAm-MeOH complex showed a structure similar to PAm-H₂O which was different from the PA-MeOH complex.³⁶

4.2 Borazine Systems

Benzene has been a molecule of considerable interest when discussing hydrogen-bonded interactions involving π systems.³⁷⁻³⁹ To see how the benzene system compares with its inorganic analogue, B₃N₃H₆, borazine, we performed hydrogen-bonded studies on the latter molecule. Borazine (BNH) was prepared in house and due to its extreme sensitivity to water, special precautions had to be adopted in its handling.⁴⁰

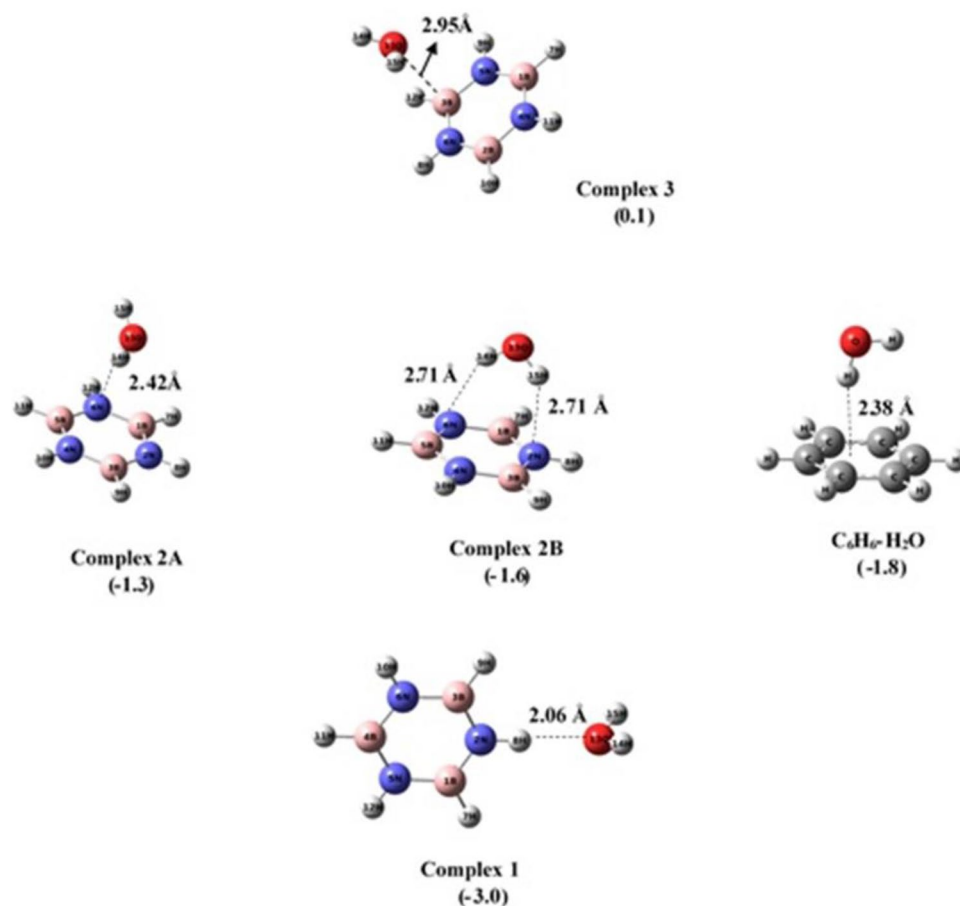


Figure 8: Optimized structures of the $B_3N_3H_6-H_2O$ complexes at the MP2/6-311++G(d,p) level. The structure of the $C_6H_6-H_2O$ complex is shown for comparison. BSSE corrected interaction energies at the MP2/6-311++G(d,p) level, in kcal/mol, is shown under each structure in parenthesis. (Reproduced from Ref. ⁴¹ with permission).

The first system that we studied was the $BNH-H_2O$ for a comparison with the $C_6H_6-H_2O$ complex.⁴¹ In contrast to the $C_6H_6-H_2O$ system, which showed only an $O-H\cdots\pi$ complex, the $BNH-H_2O$ system showed a richer landscape of structures (Fig. 8). The $BNH-H_2O$ systems showed three types of structures. The global minimum in the $BNH-H_2O$ complex was an $n-\sigma^*$ contact involving the $N-H$ of BNH and the oxygen atom of H_2O (Complex 1). There were two other local minima, one where the water was the proton donor to the nitrogen of BNH , approaching the borazine ring from above, (Complexes 2A and 2B), much like the approach of H_2O in the $C_6H_6\cdots H_2O$ complex. Another local minimum was also identified, where the oxygen of water interacted with the boron of BNH , constituting what may be regarded as the boron bond (Complex 3). However, this complex had negligible binding energy and even the sign of

the interaction energy depended on the level of theory. In our experiments, only the global minimum was observed, as indicated by the red shifts in the $N-H$ stretch of BNH (Fig. 9).⁴¹

To continue the comparison with benzene, we also studied the $BNH-C_2H_2$ system.⁴² Experimentally, we observed two complexes; one where the $N-H$ of BNH interacted with the carbon of C_2H_2 (Bent $NH\cdots C$) and another where the $\equiv C-H$ of C_2H_2 formed a hydrogen bond with the N of borazine (Bent $CH\cdots N$) (Fig. 10). In the latter complex, the approach of C_2H_2 was from above the plane of the BNH ring and resembled the most stable structure for the $C_6H_6-C_2H_2$ heterodimer. Other less stable structures corresponding to minima on the potential surface were also computed but were not observed in the experiments. All the structures are shown in Fig. 10.

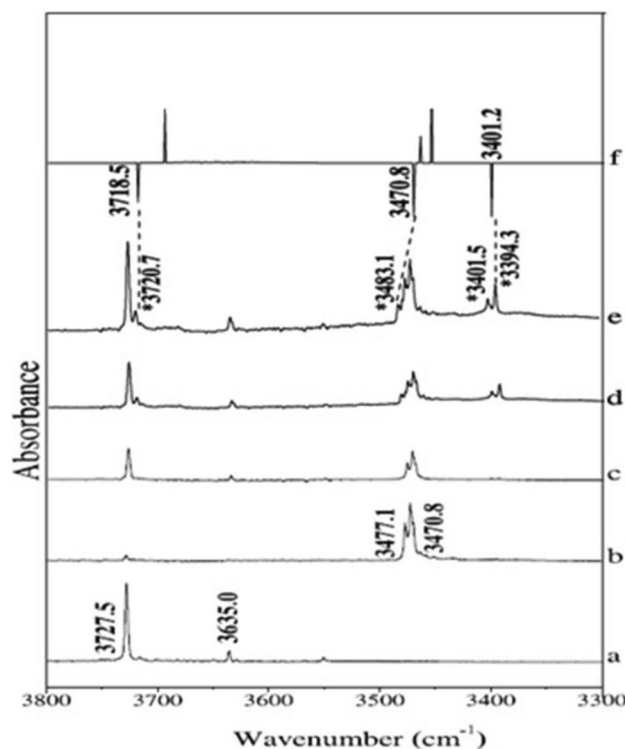


Figure 9: Spectrum of a, H₂O (3:1000); b, B₃N₃H₆ (x:1000); c, B₃N₃H₆:H₂O:N₂ (x:1:1000) at 12 K; d, spectrum of (c) annealed at 27 K; e, B₃N₃H₆:H₂O:N₂ (x:3:1000) annealed at 27 K. In all the experiments, the B₃N₃H₆ solution in tetraglyme was maintained at -20 °C. f Computed spectrum for complex 1 (down-going features) and complex 2 (up-going features). Product features in the experimental spectra are labelled with an asterisk. (Reproduced from Ref. ⁴¹ with permission).

The borazine dimer was another system that provided a very interesting comparison with the benzene dimer.⁴³ While the parallel displaced structure and the T-shaped structure are the two possible minima for the C₆H₆ dimer, the B₃N₃H₆ homodimer presents a richer landscape, as shown in Fig. 11. Two of the four structures were observed experimentally; the T_N and H⋯H structures. While the T_N structure closely resembles one of the structures of the C₆H₆ dimer, the H⋯H isomer was unique. It manifests a dihydrogen bond, two such operating cooperatively. In this bis-dihydrogen-bonded structure, the N–H group of one borazine unit interacts with H–B of another borazine molecule, while simultaneously the adjacent B–H group in the first unit interacts with an H–N group of the second. The presence of the dihydrogen-bonded dimer in our experiments was unambiguously indicated by a blue shift in the ring bending mode of B₃N₃H₆. The T_N structure was identified through red shifts in the N–H stretching mode. The report of the dihydrogen bond in the BNH dimer is one of

the few examples in a system other than a metal hydride. Another interesting aspect of the BNH dimer was that the aligned stacked structure was a minimum in addition to the parallel displaced structure. In the C₆H₆ dimer only a parallel displaced structure was a minimum and not an aligned stacked isomer.

The heterodimer, C₆H₆–B₃N₃H₆, was also studied, which showed three structures, as presented in Fig. 12.⁴⁴ One was the parallel displaced stacked structure, while the other two were nearly degenerate T-shaped isomers, with the BNH forming the stem and C₆H₆ the cap of the T. Interestingly, while in the homodimers, the stacked structures were the global minima, the T-shaped structures constituted the global minima in the BNH–C₆H₆ heterodimer.

Clearly, borazine has a mind of its own and presents a potential energy surface for its homo and heterodimers that are very different from that seen in C₆H₆.

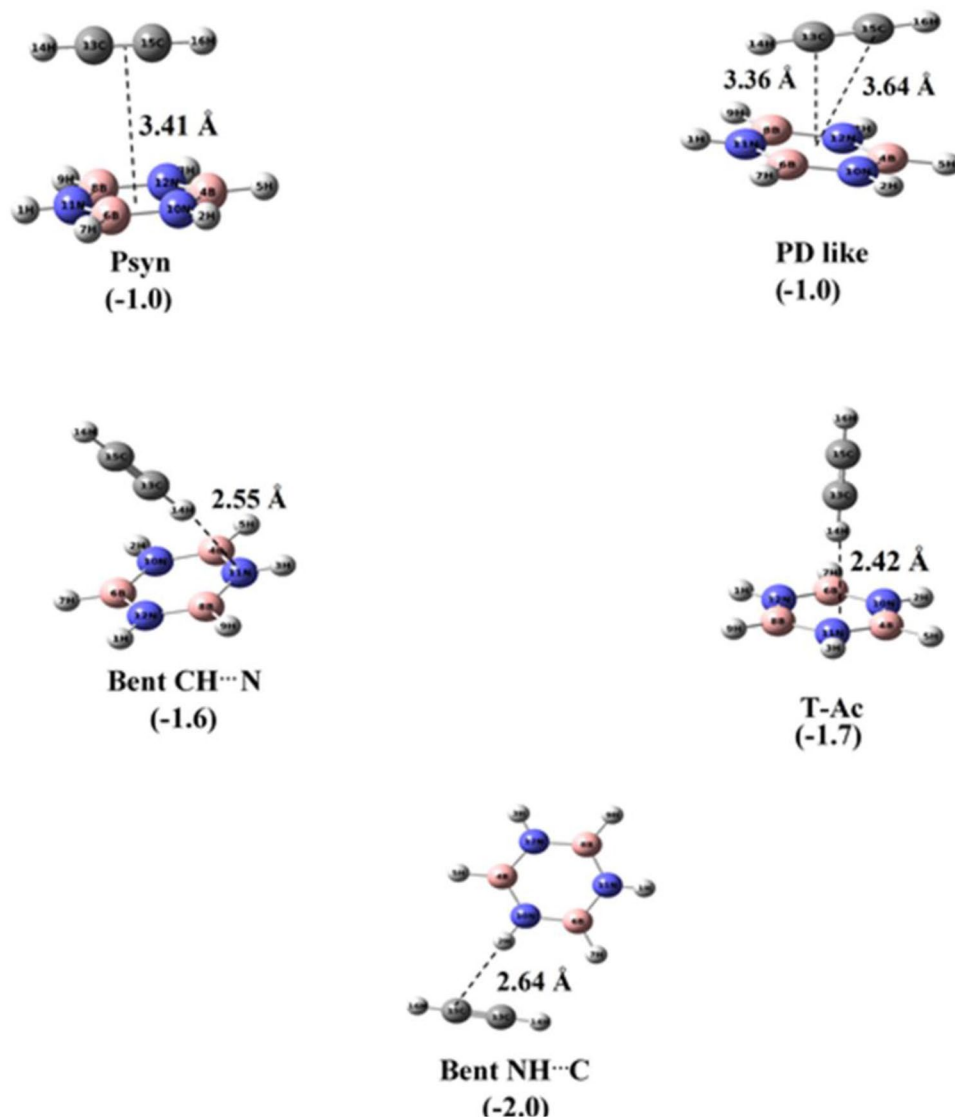


Figure 10: Optimized geometries of $B_3N_3H_6-C_2H_2$ complexes at the MP2/aug-cc-pVDZ level of theory. BSSE corrected interaction energy, in kcal/mol, computed at the MP2/aug-cc-pVDZ level, is given in parenthesis, under each structure. (Reproduced from Ref. ⁴⁰ with permission).

4.3 Interaction of Acids with Phenylacetylene

The interaction of an inorganic acid, HCl and an organic acid, HCOOH, with phenylacetylene was studied. The study of both systems yielded interesting conclusions, which are discussed in the following section.

4.3.1 Phenylacetylene–HCl Complex

The PhAc–HCl system shows a number of isomeric structures, characterized by Cl–H... π , H–Cl... π and H–Cl...H–C \equiv , all of which are shown in Fig. 13.⁴⁵ The Cl–H... π structures manifested three isomeric forms, two of which, that were nearly degenerate, involved the acetylenic π cloud

and constituted global minimum (Complexes 1a and 1b), while the third structure had a contact with the phenyl π cloud (Complex 2). All these structures were experimentally observed in the matrix, through shifts in the HCl stretch. In structure 1a, the HCl was in the plane that was inclined at an angle of 54° to the phenyl ring, while in structure 1b, the HCl was in the plane of the phenyl ring. The two structures were connected through a transition state that had HCl in a plane inclined at an angle of 22° with respect to the plane of the phenyl ring. Of course, there are other symmetry related structures, all of which are shown in Fig. 14. The barriers connecting the minima are small (0.2 kcal/mol) which allows for

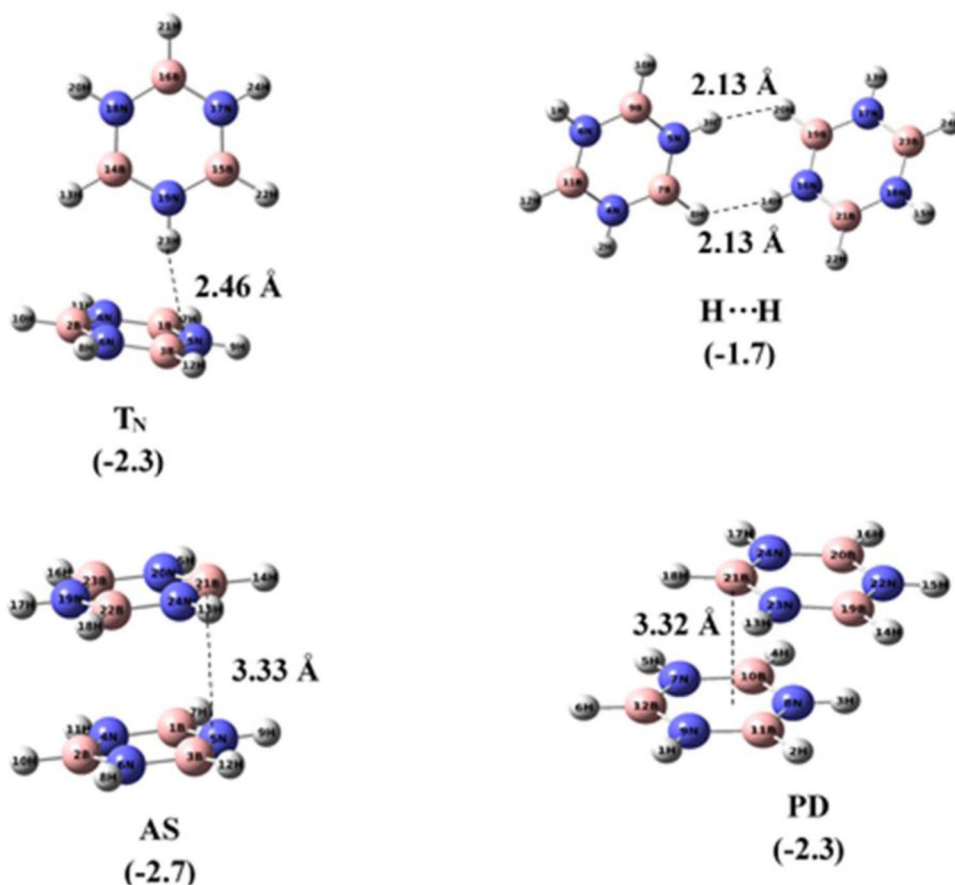


Figure 11: Optimized geometries of the $B_3N_3H_6$ homodimers computed at the MP2/aug-cc-pVDZ level. Nitrogen (blue), boron (pink) and hydrogen (white). BSSE corrected interaction energies, in kcal/mol, computed at the MP2/aug-cc-pVDZ level is given under each structure, in parenthesis. (Reproduced from Ref. ⁴³ with permission from PCCP Owner Societies).

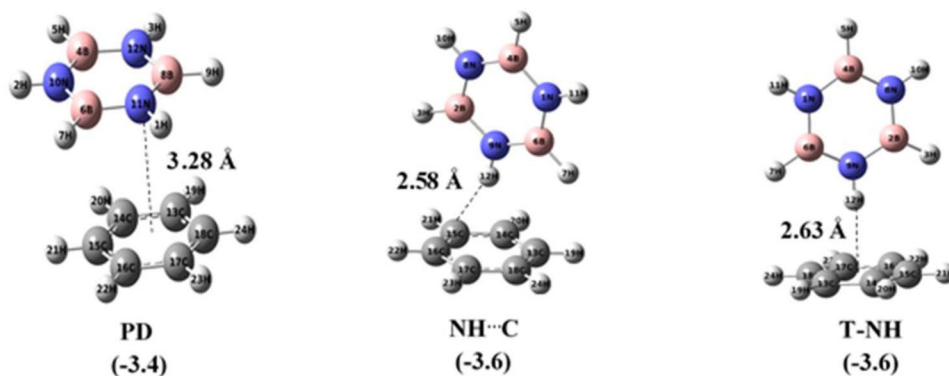


Figure 12: Optimized structures of the $B_3N_3H_6-C_6H_6$ complexes at the MP2/aug-cc-pVDZ level. The BSSE corrected energies at the same level (in kcal/mol) are given in parenthesis under each structure. (Reproduced from Ref. ⁴⁴ with permission).

a free rotation of the HCl molecule around the acetylenic stem of PhAc.

These results are relevant to the understanding of the mechanism of the HCl addition across unsaturated centres in organic molecules. It is

well known that the addition occurs in a Markovnikov fashion, through the intermediacy of a carbocation, the stability of which determines the way HCl adds across the unsaturated centre. Our computations on structures 1a and 1b

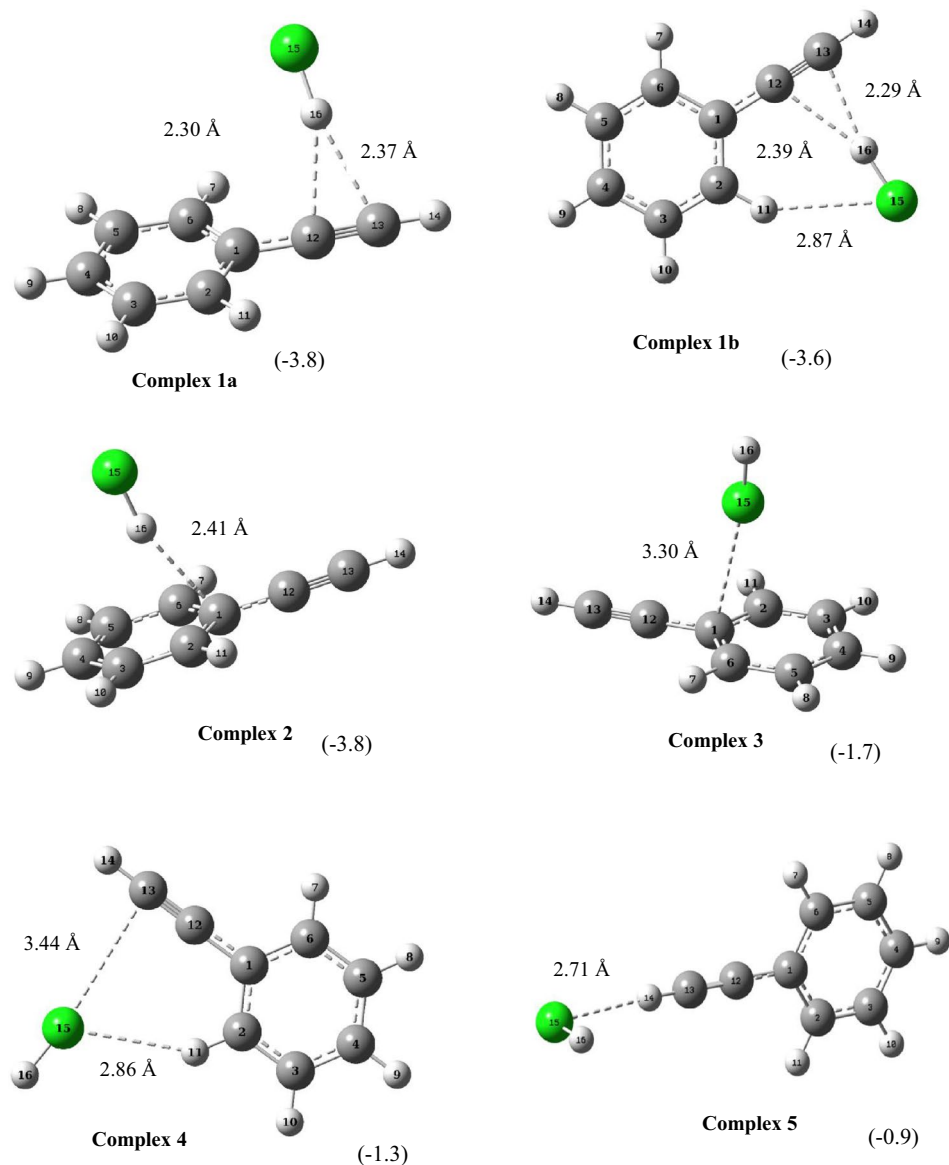


Figure 13: Optimized structures of 1:1 PhAc:HCl complexes at MP2/aug-cc-pVDZ level of theory. BSSE corrected interaction energies, in kcal/mol, calculated at the same level of theory, are given under each structure, in parenthesis. (Reproduced from Ref. ⁴⁵ with permission).

showed that the latter isomer develops a greater positive charge on the acetylenic carbon attached to the phenyl ring, compared with structure 1a. Hence structure 1b favours the incipient formation of the Markovnikov product and thus is a likely gateway structure for the addition reaction. This study provides, therefore, the micro pathway for the execution of the Markovnikov addition.

4.3.2 Phenylacetylene–HCOOH Complex

The PhAc–HCOOH yields a large number of isomeric structures (9 in number) given the multiple

binding sites for both PhAc and HCOOH.⁴⁶ In all these structures, the HCOOH was restricted to its stable trans geometry. This system can be well called a theorists' delight for the rich potential landscape it provides, but an experimentalists' nightmare. The most stable structure was composed of an O–H \cdots π_{Ac} structure together with a secondary C–H \cdots O interaction (Fig. 15), as had been discussed before with PhAc–H₂O and PhAc–MeOH systems. The two nearly degenerate structures having an O–H \cdots π_{Ac} interaction were observed unambiguously in the experiments (T2 and T3) along with a structure having O–H \cdots π_{Ph} interaction (T4).

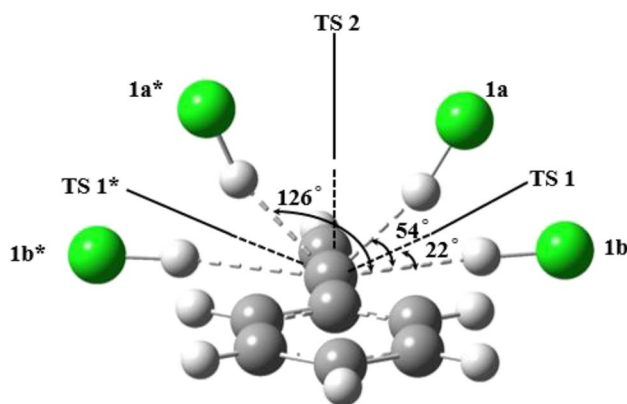


Figure 14: Depiction of various isomers of the PhAc–HCl ($H-\pi_{Ac}$) complexes together with the associated transition states, indicated by black solid lines. The angles indicate the orientation of the HCl internuclear axis with respect to the plane containing the phenyl ring. (Reproduced from Ref. ⁴⁸ with permission).

Another structure T1 was also likely observed in our experiments. All the structures T1 to T4 are shown in Fig. 15. The secondary $C-H\cdots O$ interaction in these structures involved either the $C=O$ or the OH group of *t*FA. As in the case of PhAc–HCl, here too, the *t*FA was bound rather floppily and could potentially rotate around the cylindrical acetylenic system. In fact structures T2 and T3 differed only in the orientation of the FA; in T2 the FA was in the plane of the phenyl ring while in T3, FA was oriented perpendicular to the ring. Structures with $O-H\cdots\pi_{ph}$ interactions constituted local minima. In addition to these four structures, there were five other local minima that were computed, but which are not shown here to avoid a repetitive display of structures. It can be seen that many of these structures involve multiple contacts. In spite of multiple tethers, the PhAc–*t*FA complexes appear to be floppy.

5 Can Complex Structures be Built from Simple Structures Systematically?

The study of PA– H_2O , PA–MeOH, and PA dimer systems provided an insight on developing a possible methodology to systematically arrive at the structures of complex structures starting from the structures of simpler systems, i.e., the question is can we predict the structures of PA–MeOH if we know the structures of PA– H_2O . This methodology can be understood by a reference to Fig. 16. This will be explained briefly using an example. Structure PAw1 is an optimized structure for PA– H_2O . Replacing the non-hydrogen-bonded hydrogen atom of H_2O with a methyl group yields structure PAm1, which is a minimum for

the PA–MeOH complex. Next, replacing each of the methyl hydrogen atoms in the PAm1 structure with $-C\equiv C-H$ moiety, yields three dimer structures, two of which are shown in Fig. 16 (PA_{d5} and PA_{d5B}). The third structure PA_{d6}, not shown in the figure, actually corresponds to a dimer, where one PA is in a gauche form while the second PA is in a trans structure. These guess structures were found to be close to the structures corresponding to stationary points, obtained following geometry optimization. Hence the structures of the more complicated PA dimer can be systematically derived from the relatively simpler PA– H_2O system. Likewise other structures of the PA– H_2O complexes yield corresponding structures for the PA–MeOH and PA dimer structures. This systematic procedure is reminiscent of the retrosynthetic approach used by synthetic organic chemists. A detailed presentation of this process is available in Ref. ³³.

6 Role of Hydrogen Bonds in Stabilizing Molecular Conformations

Molecular conformations derive their stability from a variety of factors such as electron delocalizations, steric factors and hydrogen bonding. Hydrogen bonding plays an important role in many cases and we will now present an example. The conformations of amino acids are an important area of study as it is very important to understand the structures of the building blocks of proteins.

Using L-threonine as an example, we will look at the conformations and discuss the role of hydrogen bonding interactions in the stability.²¹ Figure 17 depicts the various conformations of

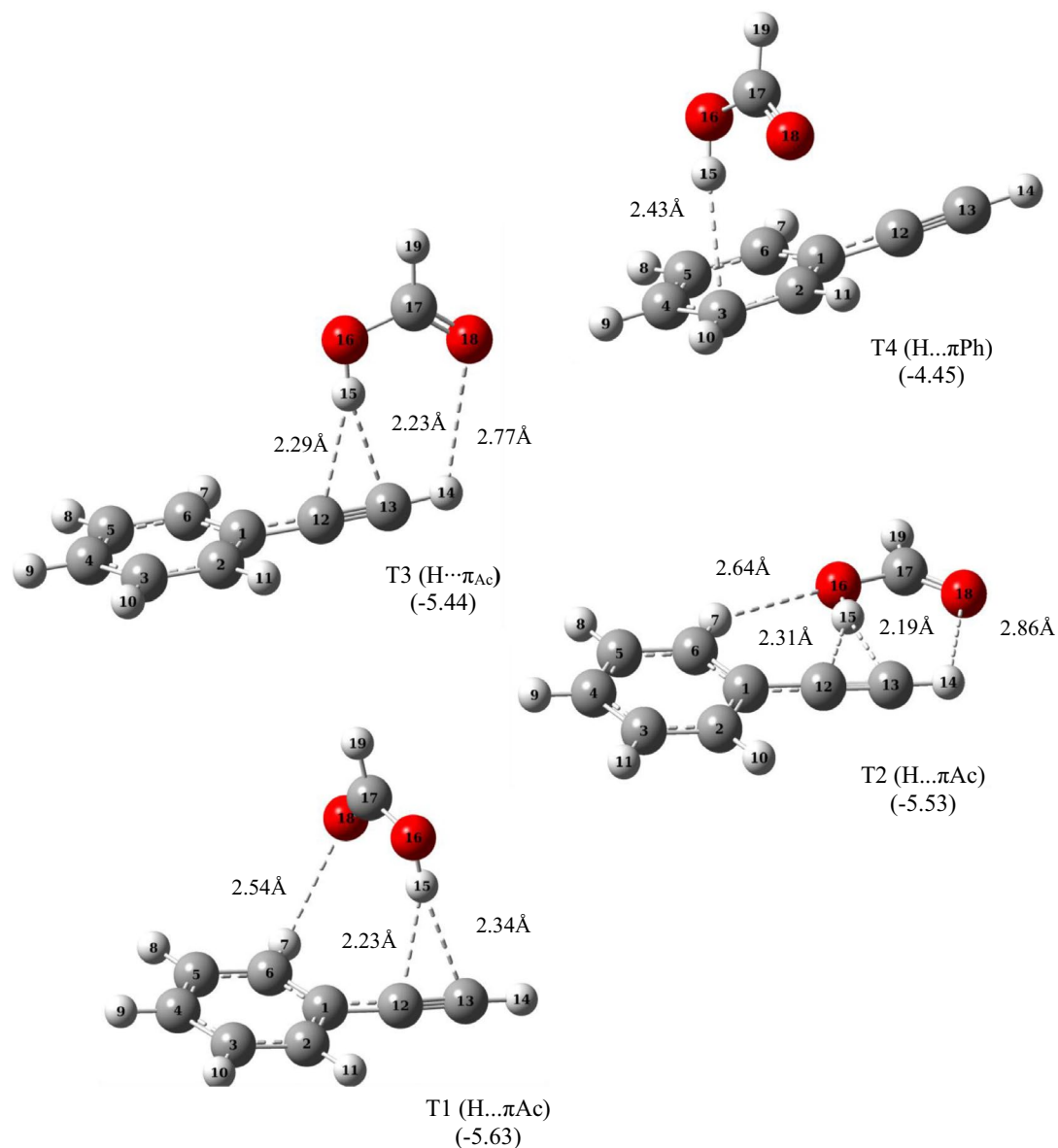


Figure 15: Optimized geometries of PhAc-tFA complexes at the MP2/aug-cc-pVDZ level, manifesting O-H... π and secondary interactions. Interaction energies, in kcal/mol, computed at CCSD(T)/CBS limit (kcal/mol) are given in parenthesis, under each structure. (Reproduced from Ref. ⁴⁶ with permission).

L-threonine. The structure THR₂₁ has a hydrogen bond between the carboxylic O-H and N of the NH₂ group. The presence of the hydrogen bond in this conformer was also evidenced experimentally as this structure has an O-H stretching frequency that is red shifted by about 119 cm⁻¹ relative to the frequency of the same mode in conformers that do not have such an intramolecular hydrogen bond. In fact, we had classified all the

conformers of the α -amino acids in eight classes based on their backbone structures, as shown in Fig. 18. The subscript in our nomenclature, while referring to the conformations of α -amino acids indicates the backbone it adopts. For example, conformer THR₂₁ indicates that conformer 2 of threonine has a Type I backbone. Type I conformers are stabilized by intramolecular hydrogen bonding interactions (Fig. 18), while all other

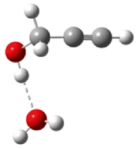
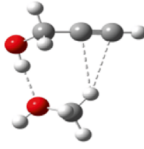
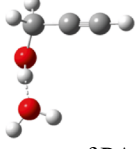
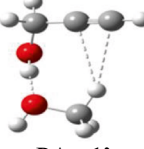
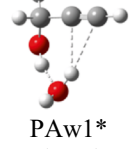
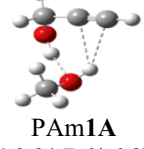
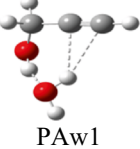
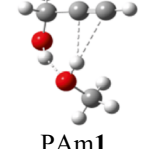
PA-H ₂ O	PA-MeOH	PA-dimers	
 Precursor of PAm1'A (Not optimized)	 PAm1'A (-7.7/-6.4/-5.7)	 PAd2B (-7.8/-6.7/-5.4)	 PAd3 (-8.9/-7.7/-6.3)
 Precursor of PAm1' (Not optimized)	 PAm1' (-8.2/-6.8/-6.3)	 PAd2 (-8.4/-7.1/-6.1)	 PAd2A (-8.3/-7.1/-6.1)
 PAw1* (-7.7/-5.7/-6.1)	 PAm1A (-9.2/-7.6/-6.8)	 PAd1 (-10.0/-8.5/-7.2)	 PAd5A (-9.3/-7.9/-6.5)
 PAw1 (-7.9/-5.9/-6.2)	 PAm1 (-9.3/-7.6/-7.0)	 PAd5 (-9.9/-8.4/-7.1)	 PAd5B (-8.8/-7.5/-6.5)

Figure 16: Correlation between the structures of PA-H₂O, PA-MeOH and PA-Dimers with their interaction energies given as $\Delta E_{\text{Raw}}/\Delta E_{\text{ZPC}}/\Delta E_{\text{BSE}}$ in kcal/mol at the MP2/aug-cc-pVDZ level. (Reproduced from Ref. 33 with permission from the Centre National de la Recherche Scientifique (CNRS) and The Royal Society of Chemistry).

structures derive their stabilities through stereo-electronic and steric effect. In earlier literature, it was proposed that a bifurcated hydrogen bonding interaction was responsible for the stability of type II structures, but we found no evidence either computationally, through AIM analysis or experimentally, through shifts in the infrared features, to assert such a stabilization. It may also be noted that even in PA it was earlier proposed that an intramolecular hydrogen bonding contact between the O-H group and the acetylenic π system was responsible for the greater stability of the gauche conformer relative to the trans structure. But our analysis has clearly shown that the gauche structure was stabilized by electronic effects and did not manifest any hydrogen bonding interaction. While hydrogen bonding interactions can certainly lead to conformer stability, the role of such interactions must be carefully analysed before arriving at such conclusions.

With regard to Fig. 18, our study on the conformations of α -amino acids showed that most of the stable structures of amino acids had either type I or II, indicating that these two were the preferred backbone structures. This is very strikingly depicted in our conformational 'dartboard', as shown in Fig. 19. Eight tracks at different radial positions on the dartboard represent eight backbone structures of α -amino acid, and all the conformations belonging to a particular backbone type fall on that corresponding track. The location of a given conformer on the appropriate track, which in turn is determined by its backbone structure is derived from the relative energy of the conformers. Beginning from the X axis, which corresponds to the lowest energy conformer, and is arbitrarily set as zero, the complete 360° is taken to represent $10.0 \text{ kcal mol}^{-1}$. Therefore, a conformer with a specific backbone structure, and an energy ΔE relative to the lowest

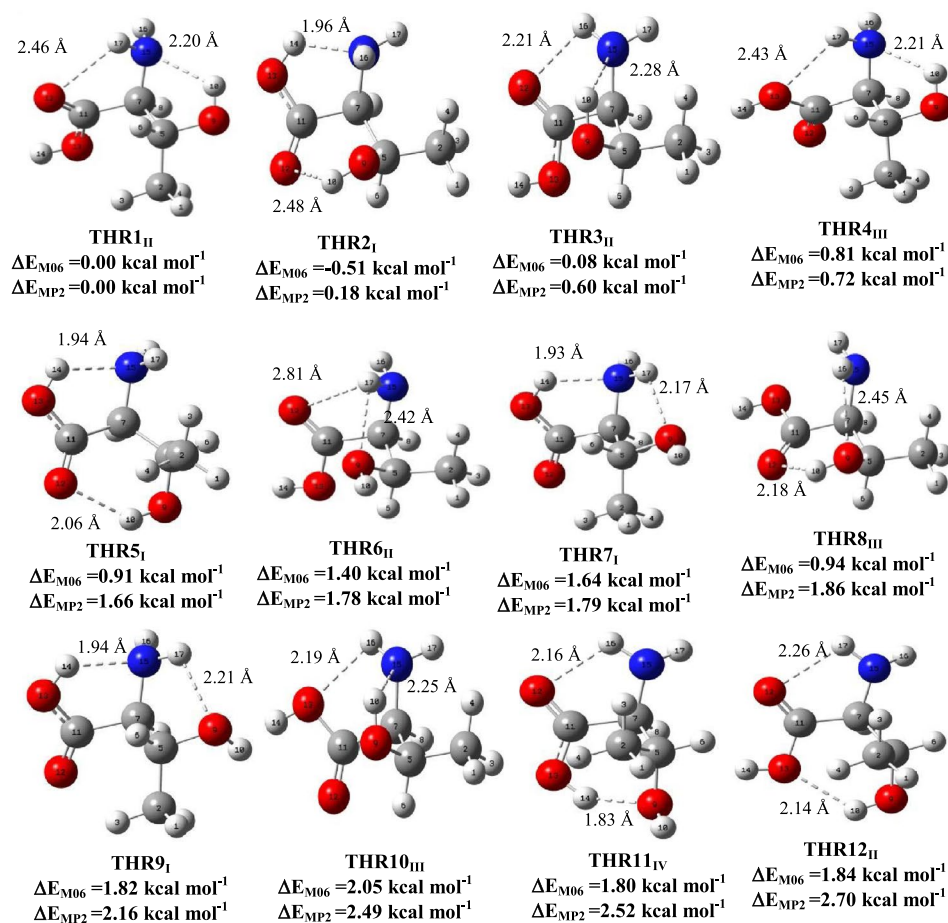


Figure 17: Optimized structures of the 12 lowest energy conformers of L-threonine at M06-2X/6-311++G(d,p) level of theory. The relative energies of the conformers, at the M06-2X/6-311++G(d,p) and MP2/6-311++G(d,p) levels, are also given, the energies being relative to the energy of THR1_{II}. (Reproduced from Ref. ²¹ with permission).

energy conformer, is positioned on the appropriate track, at an angle θ , where $\theta = \Delta E \times (360/10)$. The first octant of the dartboard (Fig. 19), which represents 1.25 kcal mol⁻¹, is observed to be predominantly populated by conformer lying on the tracks corresponding to backbone type I and II and a few to III. This observation suggests that of eight backbone structures, low energy conformers of L-threonine prefer predominantly type I, which involves a hydrogen bond, and II and rather rarely type III. Similar behavior was also observed with a few other amino acids that we studied, such as L-glutamic acid L-methionine. Computations indicated that this is a general behavior with almost all amino acids.⁴⁷

7 Conclusions

Hydrogen bonding interactions hold pride of place in directing many chemical and biological processes. The hydrogen bonding interaction is

a ubiquitous phenomenon and in spite of large number of studies, it still successfully holds the interest of the research community. Weak intermolecular interactions are responsible for crystal structures, modified reaction rates in chemistry and biology and sometimes throwing up new reaction channels. For example, the hydrogen-bonded O₃...H₂O complex is suspected to provide an additional photochemical channel for the photochemical production of the atmospheric detergent—the OH[•] radical.⁴⁸

One of the interesting aspects of our study is the competition between the various isomers and the balance tilting in favour of one isomeric form or the other depending on the subtle variations in the structure of the submolecules constituting the hydrogen-bonded complex. Our studies also revealed how multiple interactions act in a manner to optimize the stability of the complex, by adopting a compromise between the various

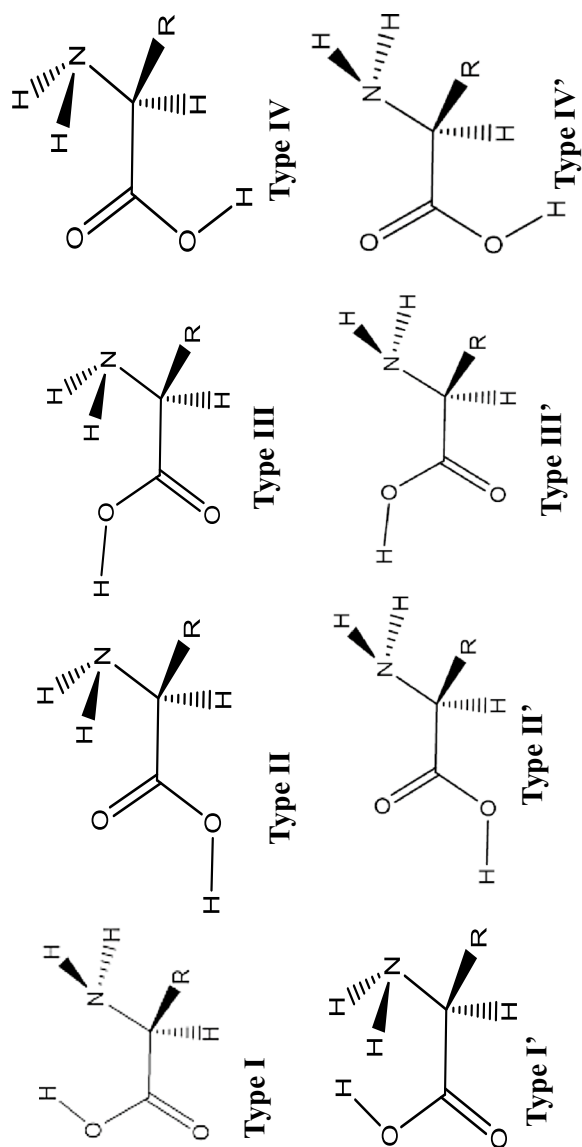


Figure 18: Eight backbone structures of α -amino acid. (Reproduced from Ref. 21 with permission).

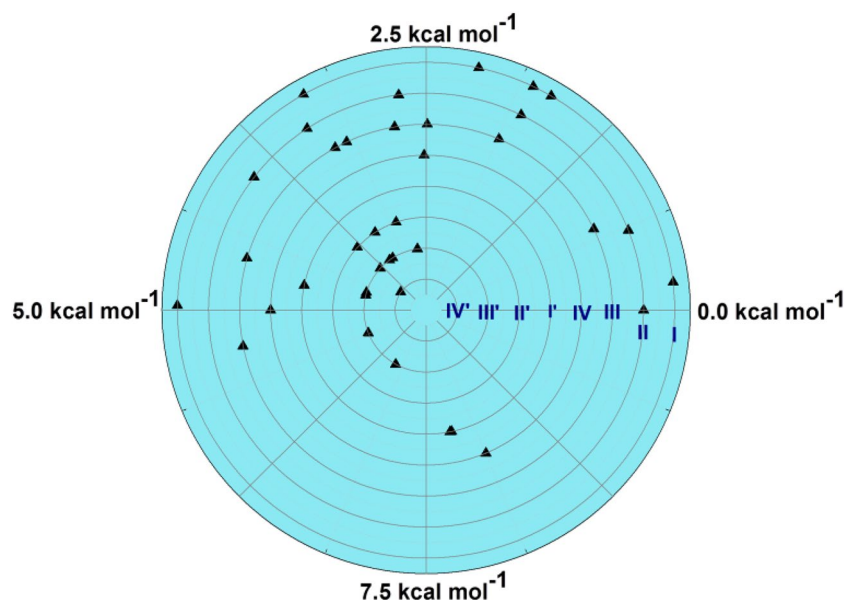


Figure 19: Conformational dartboard for 38 conformers of L-threonine at MP2/6-311++G(d,p) level of theory. (Reproduced from Ref. ²¹ with permission).

hydrogen bonding parameters. It is also apparent from our studies that structures of simpler systems could be used as templates for generating structures of more complex but related systems. We have also shown that hydrogen bonding influences the conformational landscape of amino acids, which is an important aspect in biology. Importantly it was recognized that almost all the amino acids prefer to adopt a very restricted backbone structure; an observation that could have important implications in protein structure.

Other non-covalent interactions, such as halogen bonding, carbon bonding, etc. have also demanded attention. Every study, more than providing answers, raises more questions and it can be predicted that interest in such weak interactions will remain unabated for a long time to come.

Publisher's Note

Springer Nature remains neutral with regard to jurisdictional claims in published maps and institutional affiliations.

Acknowledgements

All the authors thank IISER Mohali for the research facilities. JS, PD, KV and GK thank MHRD for research fellowships. We also acknowledge the assistance provided by various colleagues at IISER Mohali during the course of the work described in this article. The contributions of

a large number of students from IISER Mohali who had worked for their MS thesis in our group are also acknowledged. The contributions of Dr. Bishnu Prasad Kar and Dr. Anamika Mukhopadhyay are also gratefully acknowledged.

Received: 27 October 2019 Accepted: 10 December 2019

Published online: 30 December 2019

References

1. Politzer P, Murray JS, Clark T (2013) Halogen bonding and other σ^* -hole interactions: a perspective. *Phys Chem Chem Phys* 15:11178–11189
2. Mani D, Arunan E (2013) The X-C...Y (X=O/F, Y=O/S/F/Cl/Br/N/P) 'carbon bond' and hydrophobic interactions. *Phys Chem Chem Phys* 15:14377–14383
3. Zahn S, Frank R, Hey-Hawkins E, Kirchner B (2011) Pnictogen bonds: a new molecular linker? *Chem A Eur J* 17:6034–6038
4. Custelcean R, Jackson JE (2001) Dihydrogen bonding: structures, energetics, and dynamics. *Chem Rev* 101:1963–1980
5. Latimer WM, Rodebush WH (1920) Polarity and ionization from the standpoint of the Lewis theory of valence. *J Am Chem Soc* 42:1419–1433
6. Huggins MK (1919) Graduate Thesis, Univ. California, USA
7. Pauling L (1931) The nature of the chemical bond. Application of results obtained from the quantum mechanics

- and from a theory of paramagnetic susceptibility to the structure of molecules. *J Am Chem Soc* 53:1367–1400
8. Pauling L (1939) The nature of the chemical bond. Cornell University Press, Ithaca
 9. Pimentel GC, McClellan AL (1960) The hydrogen bond. Freeman, San Francisco, p 1960
 10. Steiner T (2002) The hydrogen bond in the solid state. *Angew Chem* 41:48–76
 11. Arunan E, Desiraju GR, Kline RA, Sadlej J, Schreiner S, Alkorta I, Clary DC, Crabtree RH, Dannenberg JJ, Hobza P, Kjaergaard HG, Legon AC, Mennucci B, Nesbitt DJ (2011) Definition of the hydrogen bond (IUPAC Recommendation 2011). *Pure. Appl Chem* 83:1637–1641
 12. Levy DH (1980) Laser spectroscopy of cold gas-phase molecules. *Ann Rev Phys Chem* 31:197–225
 13. Vidya V, Sankaran K, Viswanathan KS (1996) Matrix isolation-supersonic jet infrared spectroscopy, conformational cooling in trimethyl phosphate. *Chem Phys Lett* 258:113–117
 14. George L, Viswanathan KS, Singh S (1997) Ab Initio study of trimethyl phosphate: conformation analysis, dipole moments, vibrational frequencies and barriers for conformational interconversion. *J Phys Chem A* 101:2459–2464
 15. Frisch MJ, Trucks GW, H. Schlegel B, Scuseria GE, Robb MA, Cheeseman JR, Scalmani G, Barone V, Mennucci B, Peterson GA et al (2010) GAUSSIAN 09, Revision C.01, Gaussian Inc., Wallingford
 16. Boys SF, Bernardi F (1970) The calculation of small molecular interactions by the differences of separate total energies. Some procedures with reduced errors. *Mol Phys* 19:553–566
 17. Helgaker T, Klopper W, Koch H, Noga J (1997) Basis-set convergence of correlated calculations on water. *J Chem Phys* 106:9639–9646
 18. Karir G, Viswanathan KS (2016) Phenylacetylene-water complex: is it $n \cdots \sigma$ or $H \cdots \pi$ in the matrix? *J Mol Struct* 1107:145–156
 19. Verma K, Dave K, Viswanathan KS (2015) Hydrogen-bonded complexes of phenylacetylene-acetylene: who is the proton donor? *J Phys Chem A* 119:12656–12664
 20. Saini J, Viswanathan KS (2018) Does a hydrogen bonded complex with dual contacts show synergism? A matrix isolation infrared and ab initio study of the propargyl alcohol-water complex. *J Mol Struct* 1118:147–156
 21. Dubey P, Mukhopadhyay A, Viswanathan KS (2019) Do amino acids prefer only certain backbone structures? Steering through the conformational maze of L-threonine using matrix isolation infrared spectroscopy and ab initio studies. *J Mol Struct* 1175:117–129
 22. Spectra were simulated using SYNOPSIS made available by Irikura K, National Institute of Standards and Technology, Gaithersburg, MD 20899 USA (1995)
 23. Bader RFW (1994) Atoms in molecules. a quantum theory. Clarendon Press, Oxford
 24. Biegler-König F, Schönböhm J (2002) Update of the AIM2000 program for atoms in molecules. *J Comput Chem* 23:1489–1494
 25. Glendening ED, Reed AE, Carpenter JE, Weinhold F (2018) NBO Version 3.1
 26. Schmidt MW, Baldrige KK, Boatz JA, Ebert ST, Gordon MS, Jensen JH, Koseki S, Matsunaga N, Nguyen KA, Su S et al (1993) General atomic and molecular electronic structure system. *J Comp Chem* 14:1347–1363
 27. Goswami M, Arunan E (2011) Microwave spectroscopic and theoretical studies on the phenylacetylene- $\cdots H_2O$ complex: $C-H \cdots O$ and $O-H \cdots \pi$ hydrogen bonds as equal partners. *Phys Chem Chem Phys* 13:14153–14162
 28. Singh PC, Bandyopadhyay B, Patwari GN (2018) Structure of phenylacetylene-water complex as revealed by IR-UV double resonance spectroscopy. *J Phys Chem A* 112:3360–3363
 29. Jose KVJ, Gadre SR, Sundararajan K, Viswanathan KS (2007) Effect of matrix on IR frequencies of acetylene and acetylene-methanol complex: infrared matrix isolation and ab initio study. *J Chem Phys* 127:104501
 30. Engdahl A, Nelander BA (1983) The acetylene water complex, a matrix isolation study. *Chem Phys Lett* 100:129–132
 31. Frisch MJ, Pople JA, Del Bene E (1983) Hydrogen bonds between first row hydrides and acetylene. *J Chem Phys* 78:4063–4065
 32. Karir G (2018) Ph. D. Thesis, Indian Institute of Science Education & Research, Mohali, India
 33. Saini J, Viswanathan KS (2019) From the propargyl alcohol-water complex to the propargyl alcohol dimer: where does the propargyl alcohol-methanol complex fit in? *New J Chem* 43:3969–3980
 34. Saini J, Viswanathan KS (2017) Discerning near-isomeric isomers. A matrix isolation infrared and ab initio study of the propargyl alcohol dimers. *J Phys Chem A* 121:1448–1459
 35. Mani D, Arunan E (2014) Rotational spectra of propargyl alcohol dimer: a dimer bound with three different types of hydrogen bonds. *J. Chem. Phys.* 141:164311
 36. Saini J (2019) Ph. D. Thesis, Indian Institute of Science Education & Research, Mohali, India
 37. Gutowsky HS, Emilsson T, Arunan E (1993) Low-J rotational spectra, internal rotation and structures of several benzene-water dimers. *J Chem Phys* 99:4883–4893
 38. Sundararajan K, Sankaran K, Viswanathan KS, Kulkarni AD, Gadre SR (2002) $H \cdots \pi$ complexes of acetylene-benzene: a matrix isolation and computational study. *J Mol Struct* 613:209–222
 39. Majumder M, Mishra BK, Sathyamurthy N (2013) $CH \cdots \pi$ and $\pi \cdots \pi$ interaction in benzene-acetylene clusters. *Chem Phys Lett* 557:59–65
 40. Verma K (2018) Ph. D. Thesis, Indian Institute of Science Education & Research, Mohali, India

41. Mishra P, Verma K, Bawari D, Viswanathan KS (2016) Does Borazine-water behave like benzene-water? A matrix isolation infrared and ab initio study. *J. Chem. Phys.* 144:234307
42. Verma K, Viswanathan KS, Majumdar M, Sathyamurthy N (2017) How different is the borazine-acetylene dimer from the benzene-acetylene dimer? A matrix isolation infrared and ab initio quantum chemical study. *Mol Phys* 115:2637–2648
43. Verma K, Viswanathan KS (2017) The borazine dimer: the case of a dihydrogen bond competing with a classical hydrogen bond. *Phys Chem Chem Phys* 19:19067–19074
44. Verma K, Viswanathan KS (2018) “A Tale of Two Structures”: the stacks and ts of borazine and benzene hetero and homo dimers. *Chem Sel* 3:864–873
45. Karir G, Viswanathan KS (2017) H- π landscape of the phenylacetylene-HCl system: does this provide the gateway to the markovnikov addition? *J Phys Chem A* 121:5797–5808
46. Karir G, Kumar G, Kar BP, Viswanathan KS (2018) Multiple hydrogen bond tethers for grazing formic acid in its complexes with phenylacetylene. *J Phys Chem A* 122:2046–2059
47. Dubey P (2019) Ph. D. Thesis, Indian Institute of Science Education & Research, Mohali, India
48. Tsuge M, Tsuji K, Kawai A, Shibuya K (2013) Photochemistry of the ozone-water complex in cryogenic neon, argon, and krypton matrixes. *J Phys Chem A* 117:13105–13111



Jyoti Saini is currently a Teaching Assistant in the Department of Chemistry at Sardar Vallabhbhai National Institute of Technology, Surat, Gujarat, India. She obtained her integrated BS-MS degree in Chemistry from Indian Institute of Science Education and Research (IISER) Mohali, Punjab, India, in 2014. She further completed her Ph.D. from IISER Mohali in 2019. Her doctoral research work was focused on the study of conformations and hydrogen-bonded interactions in propargyl systems, using matrix isolation IR spectroscopy and ab initio computation.



Pankaj Dubey is currently a Research Associate in the Department of Chemistry, Indian Institute of Technology, Gandhinagar, Gujarat. He obtained his B.Sc. in Chemistry from Banaras Hindu University, in 2012. He then joined the Indian Institute of Science Education and Research (IISER) Mohali, in the integrated MS-Ph.D. program. He finished his Ph.D. in 2019, and his doctoral research work was focused on understanding the conformational landscape of α -amino acids and dipeptides, using matrix isolation IR spectroscopy and quantum chemistry computations.



Kanupriya Verma is currently a Visiting Scholar at the Department of Industrial and Physical Pharmacy, Purdue University, USA. She did her bachelors and masters in Chemistry from the University of Delhi, India. She completed her PhD from the Indian Institute of Science Education and Research (IISER) Mohali, Punjab, India where she looked into the hydrogen bonding interactions in various multifunctional π systems

employing matrix isolation infrared spectroscopy and ab initio calculations.



Ginny Karir is currently a post doctoral fellow in the Department of Inorganic and Physical Chemistry, Indian Institute of Science, Bengaluru. She did her Bachelors from Government College for Women, Ludhiana and Masters from Department of Chemistry, Panjab University, Chandigarh. After working as a Lecturer in her alma mater, she joined Indian Institute of Science Education and Research, Mohali, Punjab, or a PhD, where, using matrix isolation IR spectroscopy and ab initio calculations, she investigated the role reversal of phenylacetylene from proton donor to acceptor, in hydrogen bonded complexes. With Prof. Dr. Martin Suhm, at Georg-August-University Göttingen, Germany, she studied, using Slit-Jet FTIR spectroscopy, phenylacetylene as intermolecular energy balance as a benchmarking tool for quantum chemical calculations.



K. S. Viswanathan was a Professor in the Department of Chemical Sciences, IISER Mohali between 2011 and 2019. He retired from IISER in May 2019. Prior to joining IISER Mohali, he was with the Indira Gandhi Centre for Atomic Research, Department of Atomic Energy, Kalpakkam, Tamil Nadu, where he headed the Spectroscopy and Analytical Chemistry Section. His research interests are in the area of weak interactions and molecular conformations studied using matrix isolation infrared spectroscopy. He is also interested in using spectroscopic methods for trace analytical detection.